Universal thermal response of the Prussian blue lattice

T. Matsuda,[1] J. E. Kim,[1,2] K. Ohoyama,[1,3] and Y. Moritomo[1,*]
[1]*Department of Physics, University of Tsukuba, Tsukuba 305-8571, Japan*
[2]*JASRI/SPring-8, 1-1-1 Kouto, Sayo-cho, Sayo-gun, Hyogo 679-5198, Japan*
[3]*Institute for Materials Research, Tohoku University, Sendai 980-8577, Japan*
(Received 29 March 2009; revised manuscript received 6 May 2009; published 29 May 2009)

Thermal responses of Prussian blue lattice, that is, a rocksalt-type network of metal ions bridged by cyano group, are systematically investigated for $(Cs,Rb)_xM^{II}[Fe^{III}(CN)_6]_yzH_2O$ (M=Ni, Cu, Zn, and Cd) and $(Cs,Rb)_xM^{III}[Fe^{II}(CN)_6]_yzH_2O$ (M=Fe and Co) by means of the synchrotron-radiation x-ray powder diffraction. We found a universal relation between the coefficient ($\beta \equiv d \ln a/dT$; a is lattice constant) of the thermal expansion and magnitude of a: β changes the sign from positive to negative with increase in a. We ascribed the negative thermal expansion observed in the large-a region to intrinsic rotational instability of the $[Fe(CN)_6]$ unit.

DOI: 10.1103/PhysRevB.79.172302 PACS number(s): 65.40.De, 61.05.C−, 61.05.F−

Thermal expansion in crystalline materials is a relatively well-understood physical process. By virtue of the inherent anharmonicity of bond vibration, the average bond distance and hence the lattice constant increase with temperature. The coefficient ($\beta \equiv d \ln a/dT$; a is lattice constant) of the thermal expansion is usually positive and falls within the range $0 < \beta < 2 \times 10^{-5}$ K^{-1}. The sign of β, however, becomes negative in several compounds with network structure, e.g., ZrW_2O_8 (Ref. 1) and $Zn_xCd_{1-x}(CN)_2$.[2] For example, ZrW_2O_8 (Ref. 1) consists of corner-sharing ZrO_6 octahedra and WO_4 tetrahedra and exhibits negative thermal expansion ($\beta = -0.88 \times 10^{-5}$ K^{-1}) in the temperature range 0.3 K$< T <$1050 K. This unusual negative thermal response is ascribed to transverse vibration of an O atom in the W-O-Zr linkage, which effectively reduces atomic distance between W and Zr. Such a flexibility of the lattice causes interesting physical properties, such as pressure-induced structural phase transition,[3] pressure-induced amorphization,[4] and large Grüneisen parameter.[5] In addition, materials with negative thermal expansion are useful in variety of electronics application and as components of high-precision thermometers. Here, we found that the Prussian blue lattice, $A_xM[Fe(CN)_6]_yzH_2O$ (A and M are alkaline metal and metal, respectively) which consists of rocksalt-type network of metal ions bridged by cyano group (Fig. 1), exhibits a nonmonotonic change of β as a function of lattice constant a: β changes the sign from positive to negative with increase in a. Therefore, the Prussian blue lattice is an ideal platform for investigation of mechanism of the negative thermal expansion because the sign of β can be reversed by chemical substitution without changing the lattice network.

The Prussian blue family, $A_xM[Fe(CN)_6]_yzH_2O$, belongs to a face-centered cubic lattice,[6,7] except for the compounds that contain Jahn-Teller-active Mn^{III} and Cu^{II} ions. In these cases, the -NC-Fe-CN-M-NC-Fe-CN- chain makes a right angle with each other to cause a poorly packed structure; A^+ ions and H_2O molecules are accommodated in the nanopores of the network. The family is attracting current interest of material scientists due to its fruitful and sensitive response to external stimuli, such as photoexcitation,[8–13] hydrostatic pressure,[14–19] and reduced pressure.[20,21] In most cases, the response accompanies a significant structural change, suggesting an essential role of the lattice degree of freedom in these responses. The Prussian blue lattice shows curious thermal responses. For example, absolute magnitude of β are small in $RbMn^{II}[Fe^{III}(CN)_6]$ [$\beta = -0.25 \times 10^{-5}$/K (Ref. 22)], $Cs_{0.94}Mn^{II}[Fe^{III}(CN)_6]_{0.91}0.8H_2O$ [$\beta = 0.02 \times 10^{-5}$/K (Ref. 23)], and $Fe^{III}[Co^{III}(CN)_6]zH_2O$ [$\beta = -0.26 \times 10^{-5}$/K (Ref. 24)]. On the other hand, Chapman *et al.*[25] reported negative thermal expansion in a series of $M^{II}[Pt^{IV}(CN)_6]$ (M=Mn, Fe, Co, Ni, Cu, Zn, and Cd) with three-dimensional -NC-Pt-CN-M-NC-Pt-CN- network.

In this paper, we systematically investigated the thermal response in a series of Prussian blue lattice $(Cs,Rb)_xM[Fe(CN)_6]_yzH_2O$ (M=Fe, Co, Ni, Cu, Zn, and Cd), by means of the synchrotron-radiation x-ray powder diffraction. We found a universal relation between the coefficient β of the thermal expansion and magnitude of a, including the $M^{II}[Pt^{IV}(CN)_6]$ series:[25] β changes the sign from positive to negative with increase in a. The systematic change of β is ascribed to the steric confinement of the rotational displacement of the $[Fe(CN)_6]$ unit in the small-a region.

Powders of $(Cs,Rb)_xM[Fe(CN)_6]_yzH_2O$ (M=Fe, Co, Ni, Cu, Zn, and Cd) were prepared by reacting an aqueous solution of $FeCl_2$, $CoCl_2$, $NiCl_2$, $CuCl_2$, $ZnCl_2$, $CdCl_2$, RbCl, CsCl, and $K_3[Fe(CN)_6]$. Chemical compositions of the prepared samples were determined by inductively coupled plasma (ICP) and standard microanalytical methods, and are listed in Table I.

In order to precisely determine lattice constant a and space group of the above-synthesized Prussian blue analogs, x-ray powder-diffraction patterns were measured at the synchrotron-radiation facility, SPring-8. First, powder samples were filled into 0.3 mmϕ glass capillary. The capillary was put on a Debye-Scherrer camera at the BL02B2 beamline[26] of SPring-8. The wavelength of the x ray was calibrated by the lattice constant of standard CeO_2 powders. The sample temperature was controlled by cooled nitrogen gas. The exposure time was 5 min. We show in Fig. 2 typical examples of magnified x-ray diffraction patterns around (422) reflection. In Fig. 2(a) $Rb_{0.49}Co[Fe(CN)_6]_{0.80}3.8H_2O$, the (422) reflection shifts to the high-angle side with decrease in temperature, reflecting the positive (normal) ther-

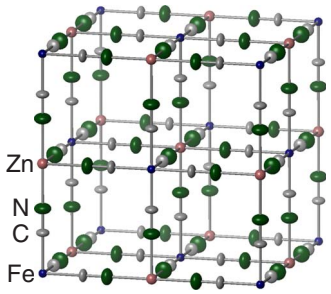

FIG. 1. (Color online) Prussian blue lattice of $Cs_{0.97}Zn[Fe(CN)_6]_{0.99}0.5H_2O$. Cs and H_2O are omitted. Displacement ellipsoids at 300 K are drawn at 80% probability level (see text).

mal expansion. In Fig. 2(b) $Cs_{1.00}Cd[Fe(CN)_6]_{1.00}0.5H_2O$, however, the (422) reflection shifts to the low-angle side with decrease in temperature, indicating the negative thermal expansion. No trace of phase separation nor impurity phase is observed in all compounds.

The lattice constants of each compounds were refined by the RIETAN-FP program[27] with the space group listed in Table I, and the normalized values were plotted in Fig. 3 against temperature: (a) $Rb_xM[Fe(CN)_6]_yzH_2O$ (M=Fe, Co, Ni, and Zn) and (b) $Cs_xM[Fe(CN)_6]_yzH_2O$ (M=Fe, Co, Ni, Cu, Zn, and Cd). The reliable factor R_I ranges from 0.97 to 5.03%. As shown by the least-square-fitted straight line, the coefficient β significantly depends on M, and even changes the sign. β is positive for M=Co, it is nearly zero for M=Ni, and Fe and is negative for M=Cu, Zn, and Cd. In Fig. 4, we plotted the coefficient β for $(Cs,Rb)_xM[Fe(CN)_6]_yzH_2O$ (M=Fe, Co, Ni, Cu, Zn, and Cd) against magnitude of a. The data points trace an universal curve (indicated by hatching), and change the sign from positive to negative with increase in a. Here, we emphasize that the universal relation is applicable even for the $M^{II}[Pt^{IV}(CN)_6]$ (Ref. 25) series (closed squares) and

TABLE I. Chemical composition, space group, lattice constant a at 300 K and coefficient ($\beta \equiv d \ln a/dT$) of the thermal expansion for $(Cs,Rb)_xM[Fe(CN)_6]_yzH_2O$ (M=Fe, Co, Ni, Cu, Zn, and Cd).

Chemical composition	Space group	a (Å)	β (10^{-5} K^{-1})
$Cs_{0.98}Fe[Fe(CN)_6]_{0.90}5.9H_2O$	$Fm\bar{3}m$	10.2561(19)	0.00
$Cs_{0.91}Co[Fe(CN)_6]_{0.84}2.0H_2O$	$Fm\bar{3}m$	9.9929(3)	+0.65
$Cs_{0.70}Ni[Fe(CN)_6]_{0.90}2.9H_2O$	$Fm\bar{3}m$	10.2915(5)	−0.04
$Cs_{0.97}Cu[Fe(CN)_6]_{0.99}1.1H_2O$	$I\bar{4}m2$	10.3946(5)[a]	−0.21
$Cs_{0.91}Zn[Fe(CN)_6]_{0.97}0.4H_2O$	$F\bar{4}3m$	10.42680(9)	−0.41
$Cs_{1.00}Cd[Fe(CN)_6]_{1.00}0.5H_2O$	$F\bar{4}3m$	10.7551(1)	−0.88
$Rb_{0.78}Fe[Fe(CN)_6]_{0.83}2.8H_2O$	$Fm\bar{3}m$	10.1986(16)	−0.21
$Rb_{0.49}Co[Fe(CN)_6]_{0.80}3.8H_2O$	$Fm\bar{3}m$	9.9431(3)	+1.46
$Rb_{0.46}Ni[Fe(CN)_6]_{0.82}4.0H_2O$	$F\bar{4}3m$	10.2562(11)	+0.01
$Rb_{0.64}Zn[Fe(CN)_6]_{0.88}2.3H_2O$	$F\bar{4}3m$	10.3924(1)	−0.59

[a]Geometrical average ($2^{1/3}a^{2/3}c^{1/3}$) of the lattice constants

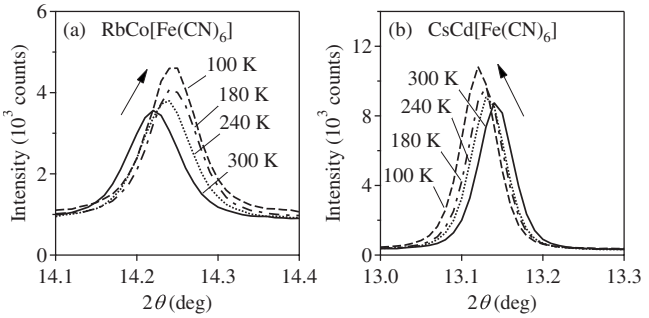

FIG. 2. Temperature dependence of magnified x-ray powder-diffraction patterns around (422) reflection for (a) $Rb_{0.49}Co[Fe(CN)_6]_{0.80}3.8H_2O$ and (b) $Cs_{1.00}Cd[Fe(CN)_6]_{1.00}0.5H_2O$. Diffraction patterns were measured in the cooling run, as indicated by arrows. X-ray wavelength was 0.5026 Å.

$Fe^{III}[Co^{III}(CN)_6]zH_2O$ (Ref. 24) (open square) with different electronic configuration from the $[Fe(CN)_6]$-based series. This universal relation indicates that the negative thermal expansion observed in large-a region should be ascribed to intrinsic instability of the Prussian blue lattice.[28,29]

In order to investigate the instability of the Prussian blue lattice, we determined the temperature variation of anisotropic atomic displacement parameter, U_{11} and U_{22}, of $Cs_{0.97}Zn[Fe(CN)_6]_{0.99}0.5H_2O$ by means of the neutron powder structural analysis. The measurements were performed using the Kinken powder diffractometer for high-efficiency and high-resolution measurements[30] (HERMES) of Institute for Materials Research, Tohoku University, installed at the JRR-3 reactor at the Japan Atomic Energy Research Agency, Tokai, Japan. Neutrons with wavelength 1.8204(5) Å were obtained by the 331 reflection of the Ge monochromator and 12′-B-Sample-22′ collimation. The powder samples were sealed in a vanadium capsule (10 mmϕ) with helium gas, and mounted at the cold head of a closed-cycle He-gas refrigerator. The diffraction data were integrated for 1.5 h. Atomic positions, occupancy g, and anisotropic atomic displacement parameter, U_{11} and U_{22}, were obtained by the Ri-

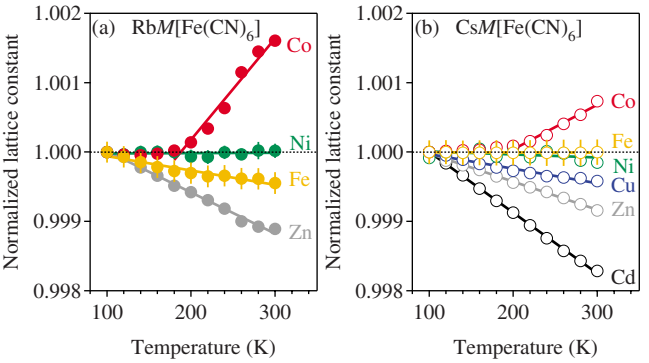

FIG. 3. (Color online) Temperature dependence of the normalized lattice constant a for (a) $Rb_xM[Fe(CN)_6]_yzH_2O$ (M=Fe, Co, Ni, and Zn) and (b) $Cs_zM[Fe(CN)_6]_yzH_2O$ (M=Fe, Co, Ni, Cu, Zn, and Cd). The chemical compositions are listed in Table I. Geometrical average ($2^{1/3}a^{2/3}c^{1/3}$) of the lattice constants was plotted for M=Cu. Straight lines are results of least-square-fittings around 300 K.

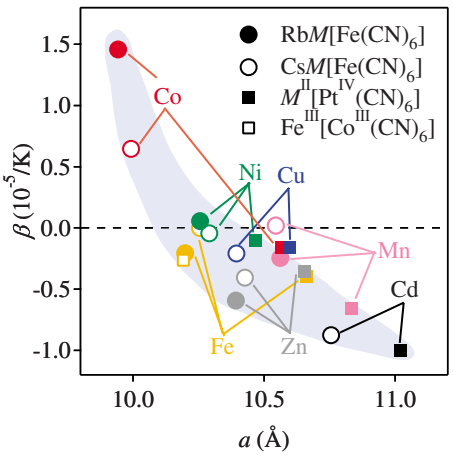

FIG. 4. (Color online) Coefficient ($\beta \equiv d \ln a/dT$) of the thermal expansion for Prussian blue lattice against a. The chemical compositions of $(Cs,Rb)_xM[Fe(CN)_6]_y zH_2O$ (M=Fe, Co, Ni, Cu, Zn, and Cd) are listed in Table I. Data points of $RbMn^{II}[Fe^{III}(CN)_6]$ and $CsMn^{II}[Fe^{III}(CN)_6]$ are cited from Refs. 22 and 23. Closed squares stand for the $M^{II}[Pt^{IV}(CN)_6]$ (M=Mn, Fe, Co, Ni, Cu, Zn, and Cd) series cited from Ref. 25. Open square stands for $Fe^{III}[Co^{III}(CN)_6]zH_2O$ cited from Ref. 24. In tetragonal compounds, geometrical average ($2^{1/3}a^{2/3}c^{1/3}$) of the lattice constants was used instead of a. Shaded area represents an universal relation between β and a.

etveld method (RIETAN-FP program[27]) with space group of $F\bar{4}3m$. We list a prototypical example of lattice parameters in Table II. In Fig. 5, we plotted the longitudinal (U_{11}: open symbol) and transversal (U_{22}: closed symbol) components of the anisotropic atomic displacement parameter for $Cs_{0.97}Zn[Fe(CN)_6]_{0.99}0.5H_2O$ against temperature. Here, we emphasize that the transversal components of the light elements (C and N) are much larger than the longitudinal components, especially at higher temperatures.

Figure 1 shows the displacement ellipsoids drawn at 80%

TABLE II. Atomic positions, occupancy g and anisotropic atomic displacement parameter, U_{11} and U_{22}, of $Cs_{0.97}Zn[Fe(CN)_6]_{0.99}0.5H_2O$ at 100 K determined by neutron powder structural analysis. The crystal symmetry is face-centered cubic ($F\bar{4}3m$;Z=4) with a=10.437 06(12) Å. U_{11} of Cs2 is fixed at the value of Cs1. Atomic position and atomic displacement parameters of O are fixed at the values of N. g of Cs1 is fixed at the value determined from the 300 K diffraction pattern. Reliable factors R_I is 1.62%.

Atom	Site	g	x	y	z	U_{11} (Å^2)	U_{22} (Å^2)
Fe	4a	0.99	0	0	0	0.0028(7)	
Zn	4b	1	1/2	0	0	0.0051(10)	
Cs1	4c	0.71	1/4	1/4	1/4	0.0147(14)	
Cs2	4d	0.26	3/4	3/4	3/4	0.0147	
C	24f	0.99	0.18478(11)	0	0	0.0031(11)	0.0096(5)
N	24f	0.99	0.29572(10)	0	0	0.0077(7)	0.0151(5)
O	24f	0.01	0.29572	0	0	0.0077	0.0151

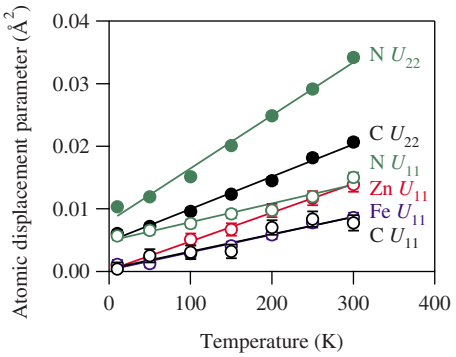

FIG. 5. (Color online) Temperature variation of anisotropic atomic displacement parameter, U_{11} and U_{22} of $Cs_{0.97}Zn[Fe(CN)_6]_{0.99}0.5H_2O$. Open and closed symbols represent longitudinal (U_{11}) and transversal (U_{22}) components, respectively. Solid lines are least-square-fitted results.

probability level for $Cs_{0.97}Zn[Fe(CN)_6]_{0.99}0.5H_2O$ at 300 K. One may notice that the transversal atomic displacement of N is larger than that of C, which suggests that the transversal displacement of the light elements can be ascribed to the thermally excited rotational displacement (or rotational disorder) of the $[Fe(CN)_6]$ unit. With such a rotational motion of the $[Fe(CN)_6]$ unit, atomic distance between Zn and Fe effectively reduces. Thus, the rotational displacement causes the negative thermal expansion as observed. The rotational motion should be enhanced in the large-a region with sufficient open space for atomic displacement, but be suppressed in the small-a region by steric confinement. This scenario qualitatively explains the empirical relation between β and a (see Fig. 4). The present scenario is further supported by temperature variation of Raman-scattering spectra of $Rb_{0.85}Zn[Fe(CN)_6]_{0.95}1.5H_2O$. The CN stretching modes show softening with temperature: temperature coefficient ($d\hbar\omega/dT$) of the Raman shift is -0.0188 cm^{-1}/K (-0.0183 cm^{-1}/K) for the $A_{1g}(E_g)$ mode. The observed softening of the CN stretching vibration suggests that the local Zn-N/Fe-C bond distances effectively elongate with temperature. Thus, the Prussian blue lattice has the intrinsic rotational instability of the $[Fe(CN)_6]$ unit.

The instability of the Prussian blue lattice is considered to be a key factor for deeper understanding of the fruitful and sensitive response to the external stimuli, such as photoexcitation[8–13] and hydrostatic pressure.[14–19] For example, Kamioka *et al.*[12,13] reported that lifetime of the photocreated charge-transferred state in $Mn^{II}[Fe^{III}(CN)_6]_{2/3}5H_2O$, $Fe^{III}[Fe^{II}(CN)_6]_{3/4}3.5H_2O$, and $Co^{II}[Fe^{III}(CN)_6]_{2/3}5H_2O$ is pretty long (~1 ns) at 300 K. Such a long lifetime can be ascribed to the strong coupling between the charge transfer, i.e., $Mn^{II} \rightarrow Fe^{III}$, $Fe^{II} \rightarrow Fe^{III}$, and $Co^{II} \rightarrow Fe^{III}$, and the lattice system, especially the rotational displacement of the $[Fe(CN)_6]$ unit. Because the electron-lattice coupling would stabilize the charge-transferred state by the local lattice distortion. On the other hand, Liu *et al.*[17] reported pressure-induced octahedral rotation in $RbMn[Fe(CN)_6]$ at 2.0 GPa by means of the high-pressure Raman-scattering spectroscopy. They further found similar phenomena in $Rb_{0.85}Zn[Fe(CN)_6]_{0.95}1.5H_2O$ at 1.1

GPa and in $Rb_{0.64}Zn[Fe(CN)_6]_{0.88}1.5H_2O$ at 1.7 GPa.[31] These pressure-induced structural phase transitions may be regarded as a cooperative freezing of the rotational mode of the $[Fe(CN)_6]$ unit.

In summary, we found a universal relation between β and a in a series of the Prussian blue lattice, $(Cs,Rb)_xM[Fe(CN)_6]_yzH_2O$ (M=Fe, Co, Ni, Cu, Zn, and Cd). The universal relation together with the anisotropic displacement parameters of cyano group indicates that the Prussian blue lattice has the intrinsic rotational instability of the $[Fe(CN)_6]$ unit. We ascribed the universal relation between β and a to the steric confinement of the rotational displacement in the small-a region. We believe that the intrinsic lattice instability is a key factor for deeper understanding of the fruitful and sensitive response to the external stimuli, such as photoexcitation and hydrostatic pressure. We emphasize that the Prussian blue lattice is an ideal platform for investigation of mechanism of the negative thermal expansion because the thermal response can be reversed by chemical substitution.

We are grateful to H. Kamioka and X. J. Liu for their help in Raman-scattering experiment, and to K. Nemoto for his help in the neutron powder experiment. This work was supported by a Grant-In-Aid for Scientific Research from the Ministry of Education, Culture, Sports and Science and from the Support Center for Advanced Telecommunication (SCAT) foundation. The synchrotron-radiation x-ray powder-diffraction experiments were performed at the SPring-8 BL02B2 beamline with approval of the Japan Synchrotron Radiation Research Institute (JASRI). T.M. is supported by the Inoue Foundation of Science. Elementary analysis of the films was performed at the Chemical Analysis Division, Research Facility Center for Science and Engineering, University of Tsukuba.

*Author to whom correspondence should be addressed.

[1] T. A. Mary, J. S. Evans, T. Vogt, and A. W. Sleight, Science **272**, 90 (1996).
[2] A. L. Goodwin, and C. J. Kepert, Phys. Rev. B, **71**, 140301(R) (2005).
[3] J. O. S. Evans, Z. Hu, H. D. Jorgensen, D. N. Argyriou, S. Short, and A. W. Sleight, Science **275**, 61 (1997).
[4] C. A. Perottoni and J. A. H. da Jornada, Science **280**, 886 (1998).
[5] R. Mittal, S. L. Chaplot, H. Schober, and T. A. Mary, Phys. Rev. Lett. **86**, 4692 (2001).
[6] A. Ludi and H. U. Güdel, in *Structural Chemistry of Polynuclear Transition Metal Cyanides*, edited by D. J. Dunitz *et al.*, Structure & Bonding, Vol. 14 (Springer, Berlin, 1973), p. 1–21.
[7] F. Herren, P. Fischer, A. Ludi, and W. Halg, Inorg. Chem. **19**, 956 (1980).
[8] O. Sato, T. Iyoda, A. Fujishima, and K. Hashimoto, Science **272**, 704 (1996).
[9] H. Tokoro, S. Ohkoshi, and K. Hashimoto, Appl. Phys. Lett. **82**, 1245 (2003).
[10] D. A. Pejaković, J. L. Manson, J. S. Miller, and A. J. Epstein, Phys. Rev. Lett. **85**, 1994 (2000).
[11] Y. Moritomo, F. Nakada, H. Kamioka, T. Hozumi, and S. Ohkoshi, Phys. Rev. B **75**, 214110 (2007).
[12] H. Kamioka, Y. Moritomo, W. Kosaka and S. Ohkoshi, Phys. Rev. B **77**, 180301(R) (2008).
[13] H. Kamioka, Y. Moritomo, W. Kosaka, and S. Ohkoshi, J. Phys. Soc. Jpn. **77**, 093710 (2008).
[14] L. Egan, K. Kamenev, D. Papanikolaou, Y. Takabayashi, and S. Margadonna, J. Am. Chem. Soc. **128**, 6034 (2006).
[15] E. Coronado, M. C. Giménez-Lopez, T. Korzeniak, G. Levchenko, F. M. Romero, A. Segura, V. Garcia-Baonza, J. C. Cezar, F. M. F. de Groot, A. Milner, and M. Paz-Pasternak, J. Am. Chem. Soc. **130**, 15519 (2008).
[16] V. Ksenofontov, G. Levchenko, S. Reiman, P. Gütlich, A. Bleuzen, V. Escax, and M. Verdaguer, Phys. Rev. B **68**, 024415 (2003).
[17] X. J. Liu, Y. Moritomo, T. Matsuda, H. Kamioka, H. Tokoro, and S. Ohkoshi, J. Phys. Soc. Jpn. **78**, 013602 (2008).
[18] Y. Moritomo, M. Hanawa, Y. Ohishi, K. Kato, M. Takata, A. Kuriki, E. Nishibori, M. Sakata, S. Ohkoshi, H. Tokoro, and K. Hashimoto, Phys. Rev. B **68**, 144106 (2003).
[19] M. Hanawa, Y. Moritomo, A. Kuriki, J. Tateishi, K. Kato, M. Takata, and M. Sakata, J. Phys. Soc. Jpn. **72**, 987 (2003).
[20] Y. Moritomo, F. Nakada, J. E. Kim, and M. Takata, Appl. Phys. Express **1**, 111301 (2008).
[21] Y. Moritomo, F. Nakada, H. Kamioka, J. E. Kim, and M. Takata, Appl. Phys. Lett. **92**, 141907 (2008).
[22] Y. Moritomo, K. Kato, A. Kuriki, M. Takata, M. Sakata, H. Tokoro, S. Ohkoshi, and K. Hashimoto, J. Phys. Soc. Jpn. **71**, 2078 (2002).
[23] T. Matsuda, H. Tokoro, K. Hashimoto, and S. Ohkoshi, Dalton Trans. (2006) 5046.
[24] S. Margadonna, K. Prassides, and A. N. Fitch, J. Am. Chem, Soc. **126**, 15390 (2004).
[25] K. W. Chapman, P. J. Chupas, and C. J. Kepert, J. Am. Chem, Soc. **128**, 7009 (2006).
[26] E. Nishibori, M. Takata, K. Kato, M. Sakata,Y. Kubota, S. Aoyagi, Y. Kuroiwa, M. Yamakata, and N. Ikeda, Nucl. Instrum. Methods Phys. Res. A **467-468**, 1045 (2001).
[27] F. Izumi and K. Momma, Solid State Phenom. **130**, 15 (2007).
[28] No correlation is observed between β and chemical composition of the compounds, i.e., x (alkaline metal concentration), y ($[Fe(CN)_6]$ concentration), and z (water concentration).
[29] We think that magnetic interaction between transition metals has no relation with the lattice response because magnetic transition temperatures of transition metal hexacyanoferrates are known to be below ~30 K.
[30] K. Ohoyama, T. Kanouchi, K. Nemoto, M. Ohashi, T. Kajitani, and Y. Yamaguchi, Jpn. J. Appl. Phys., Part 2 **37**, 3319 (1998).
[31] X. J. Liu and Y. Moritomo (private communication).